Figure S1

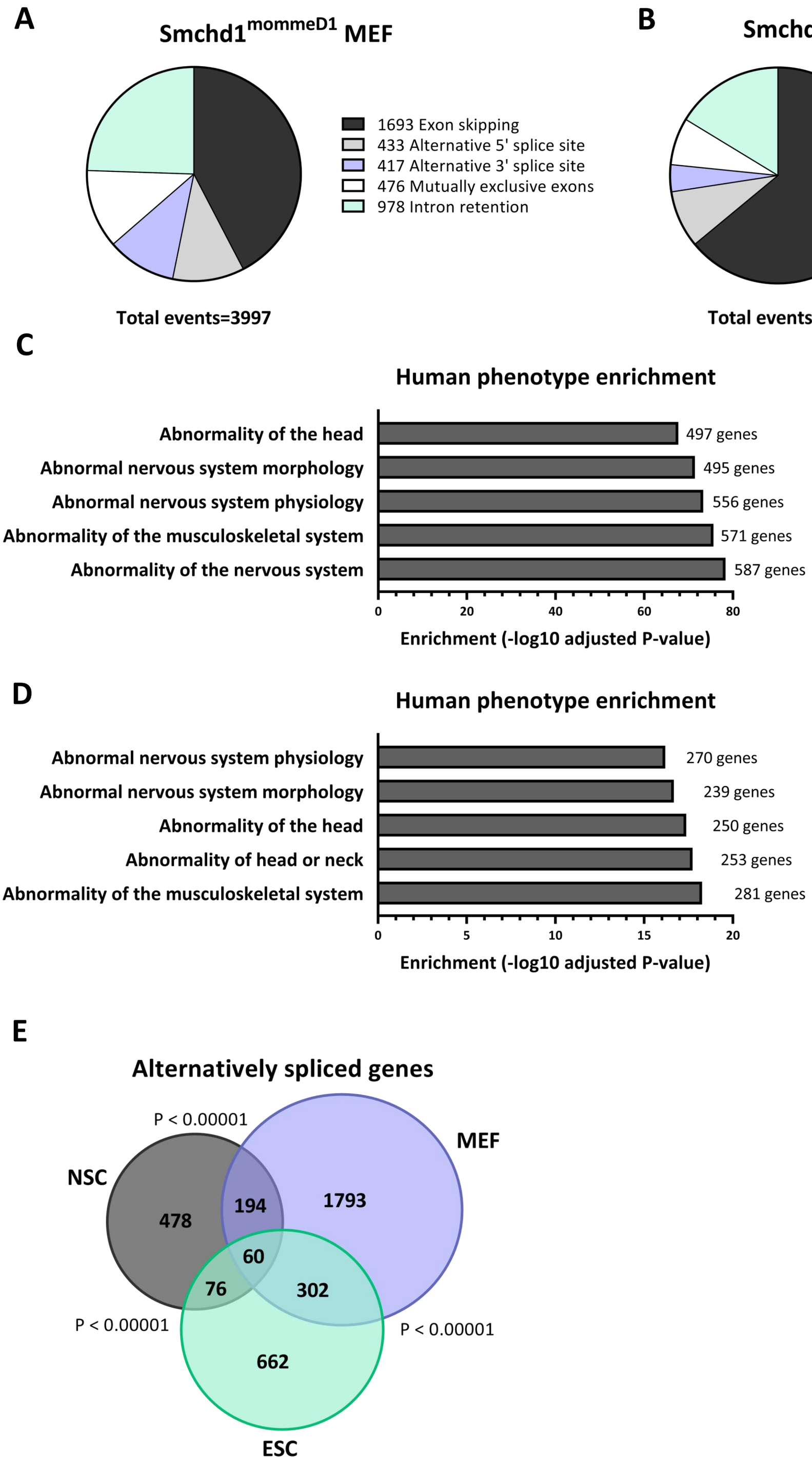

Figure S1. A-E. RNA-seq of Smchd1^{MommeD1} MEF **(A,C)** and Smchd1-KO mESC **(B,D)** samples was analyzed using rMATS (FDR<0.05). Proportion of each alternative splicing event is presented relative to WT , summary of significant alternative splicing events (FDR<0.05) from the five subtypes identified by rMATS in Smchd1^{MommeD1} mice MEF **(A)** and mESC **(B)** RNA-seq data . Top five significant events for human phenotype gene set, enrichment significance represented as –log10 adjusted P-value. **(C-D).** ***E.*** Venn diagram presenting the overlap between Smchd1 alternative splicing regulation in NSC, ESC and MEF of Smchd1 null or Smchd1-KO mice.

Figure S2

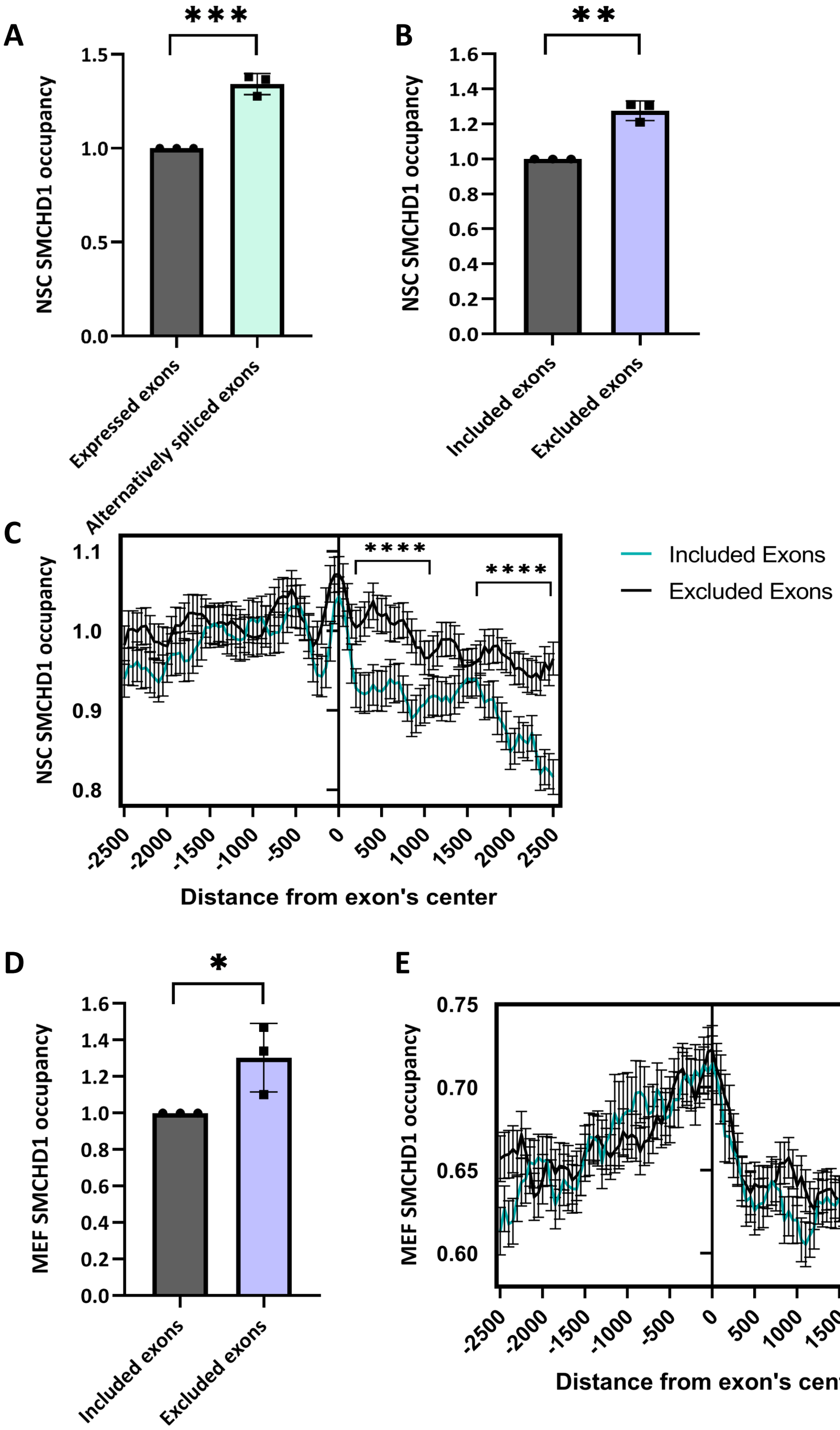

Figure S2

A-C GFP ChIP-seq in primary NSCs with endogenous Smchd1-GFP fusion protein. Smchd1 occupancy analyzed as the number of Smchd1 peaks present within 5kb of alternatively spliced or expressed (TPM>1) exons **(A)** or within 5kb of differentially included or excluded exons in Smchd1^{MommeD1} NSC **(B)** .Values represent averages of three ChIP-seq replicates from each cell type ±SD [* p<0.05; **p<0.01; ***p<0.001;]. Aggregation plot depicting the average normalized Smchd1 occupancy, at and near exons differentially included or excluded in Smchd1^{MommeD1} mice. X axis represent bins of size 50 bp around the center of the exon [****p<0.0001] **(C)**. ***D-E.*** SMCHD1 ChIP-seq in MEFs. SMCHD1 occupancy analyzed as the number of SMCHD1 peaks present within 5kb of included or excluded exons in Smchd1^{MommeD1} MEF. Values represent averages of three ChIP-seq replicates from each cell type ±SD [* p<0.05; **p<0.01; ***p<0.001;] (A). Aggregation plot depicting the average normalized Smchd1 occupancy, at and near exons differentially included or excluded in Smchd1^{MommeD1} MEF. X axis represent bins of size 50 bp around the center of the exon [**p<0.01].

Figure S3

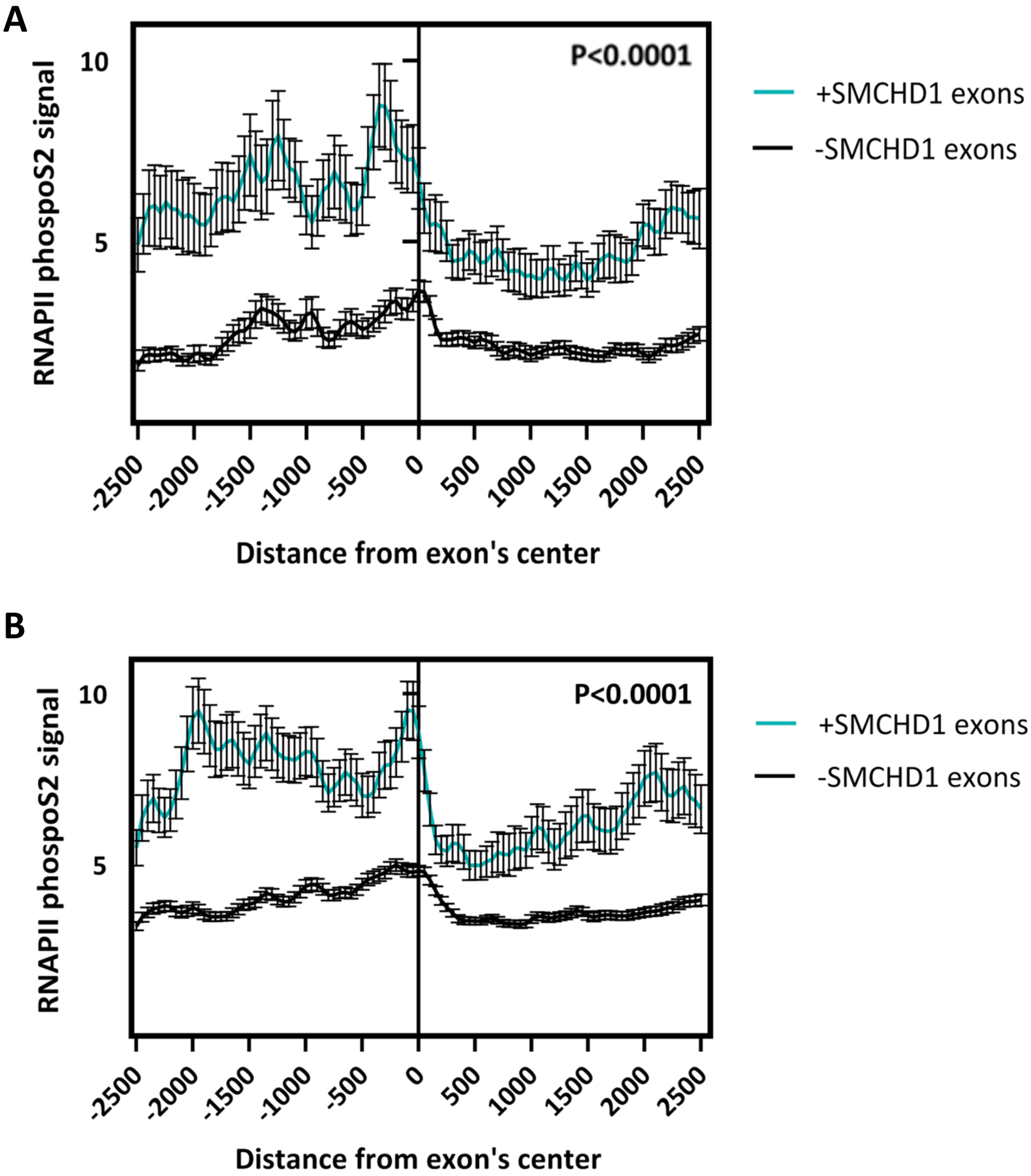

Figure S3

A-B. Aggregation plot depicting the average normalized phospho-Ser2 levels of RNAPII at and near alternatively spliced exons differentially bound by Smchd1 in NSC (A) or MEF (B). X axis represent bins of size 50 bp around the center of the exon .

Figure S4

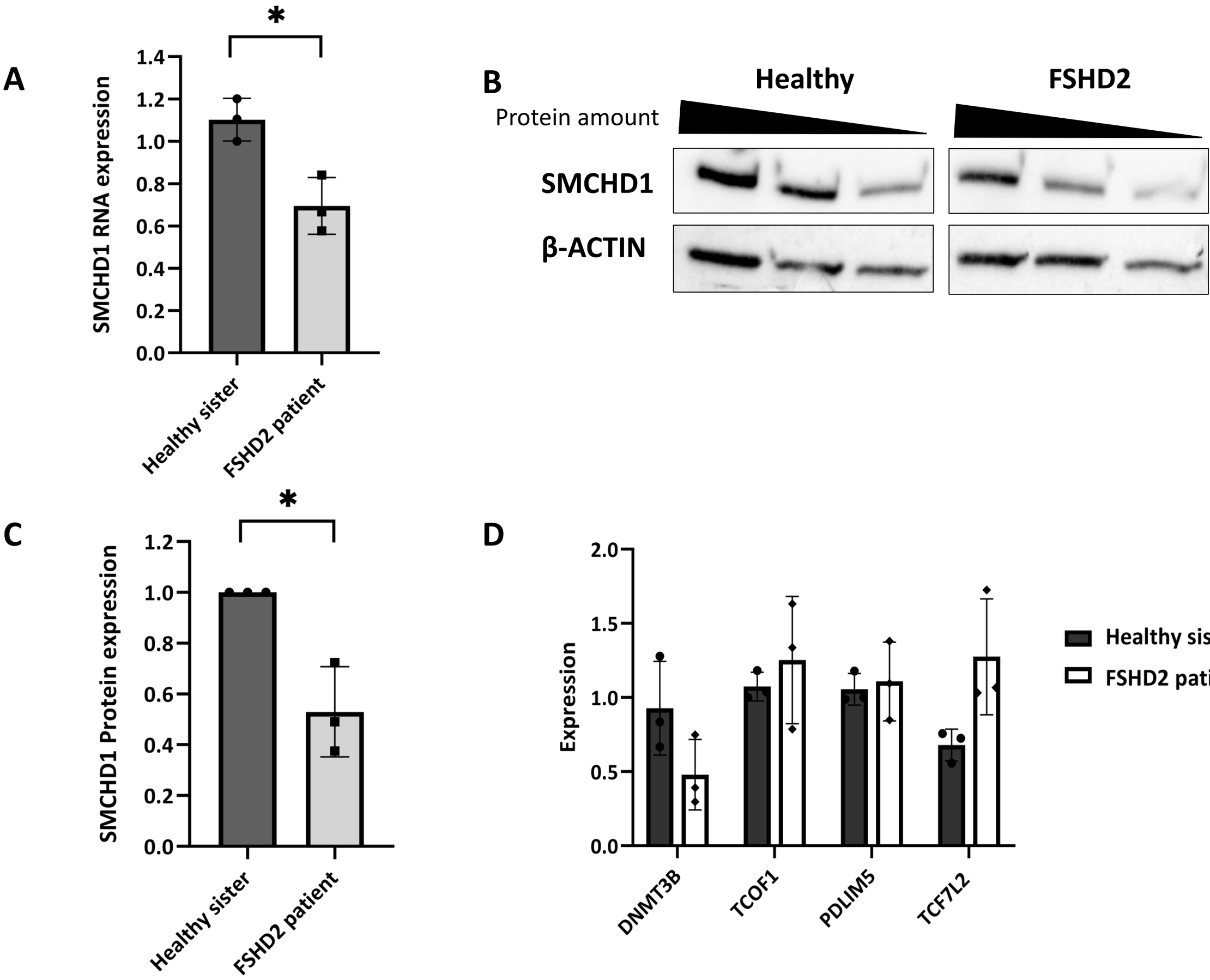

Figure S4. A-D. RNA was extracted from lymphoblasts of an FSHD2 patient and her healthy sister and analyzed by real-time PCR for *SMCHD1* total mRNA amount relative to *CycloA* reference gene (**A**). Protein was extracted and Western blot was conducted with the indicated antibodies **(B**). Quantification of Western blot **(C)**. RNA was extracted and real-time PCR was conducted to the indicated gene relative to *CycloA* reference gene (**D**). Values represent averages of three experiments ±SD, [* $p<0.05$].

Figure S5

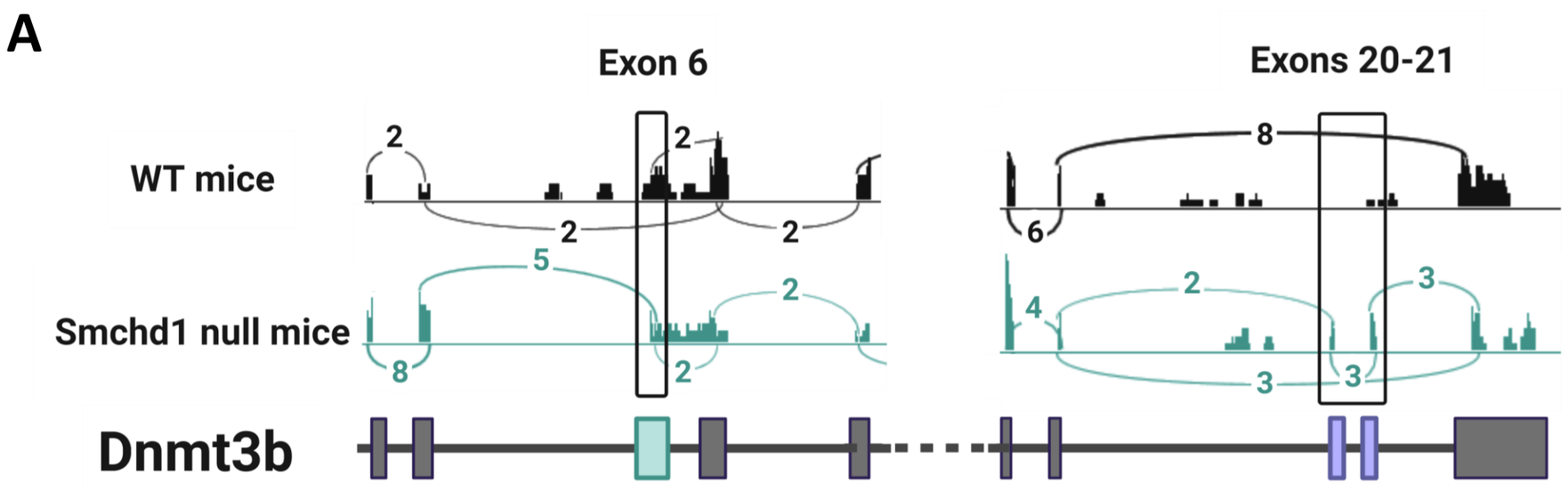

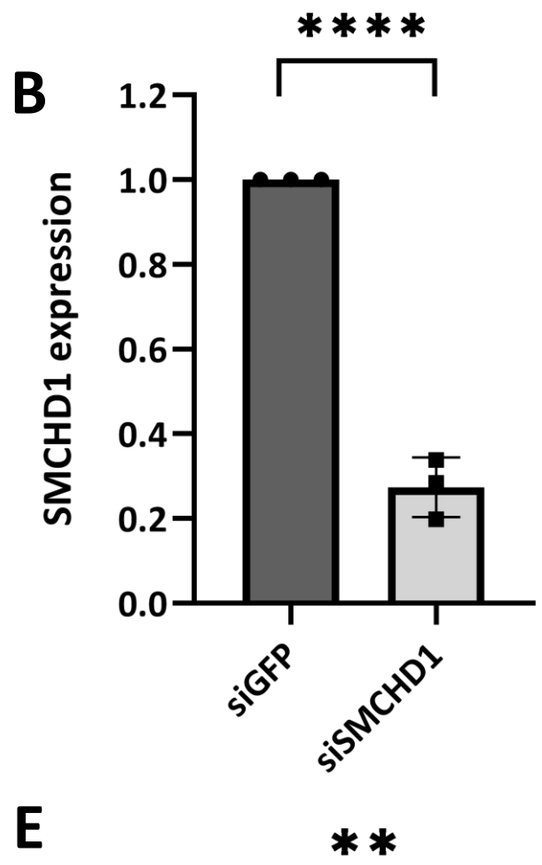

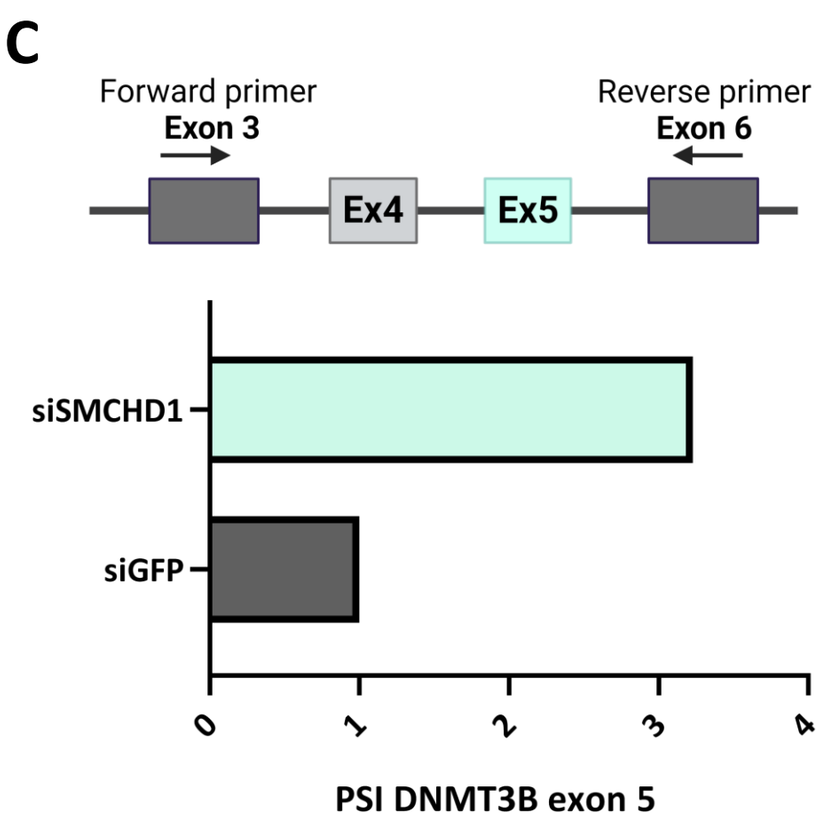

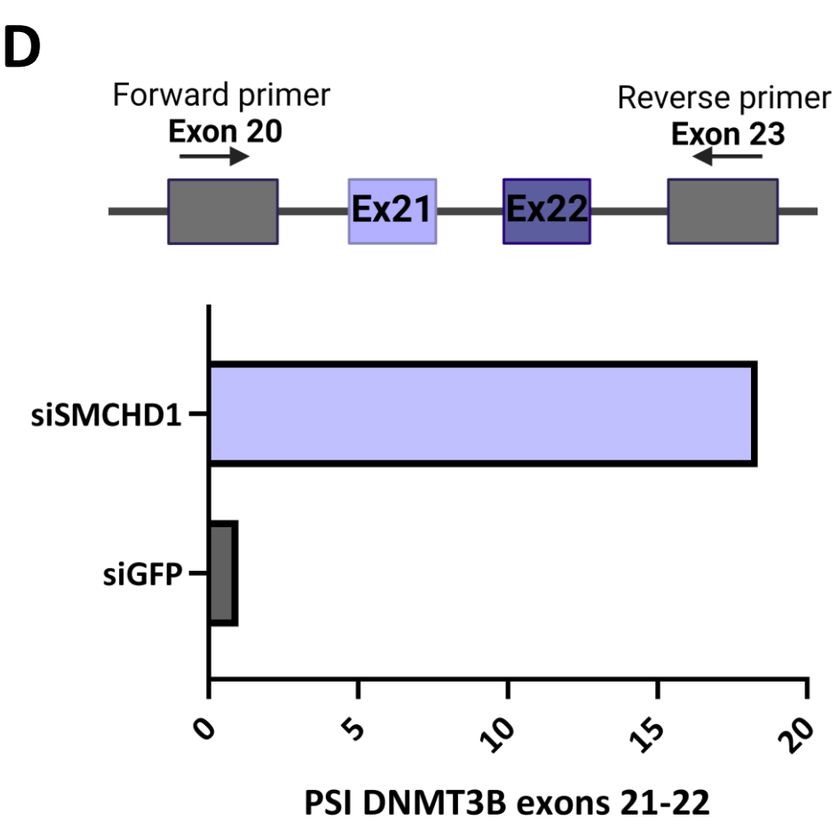

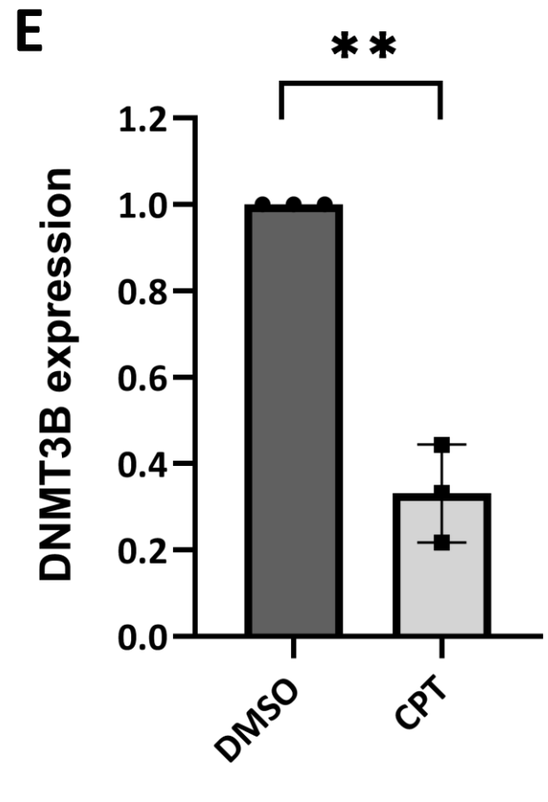

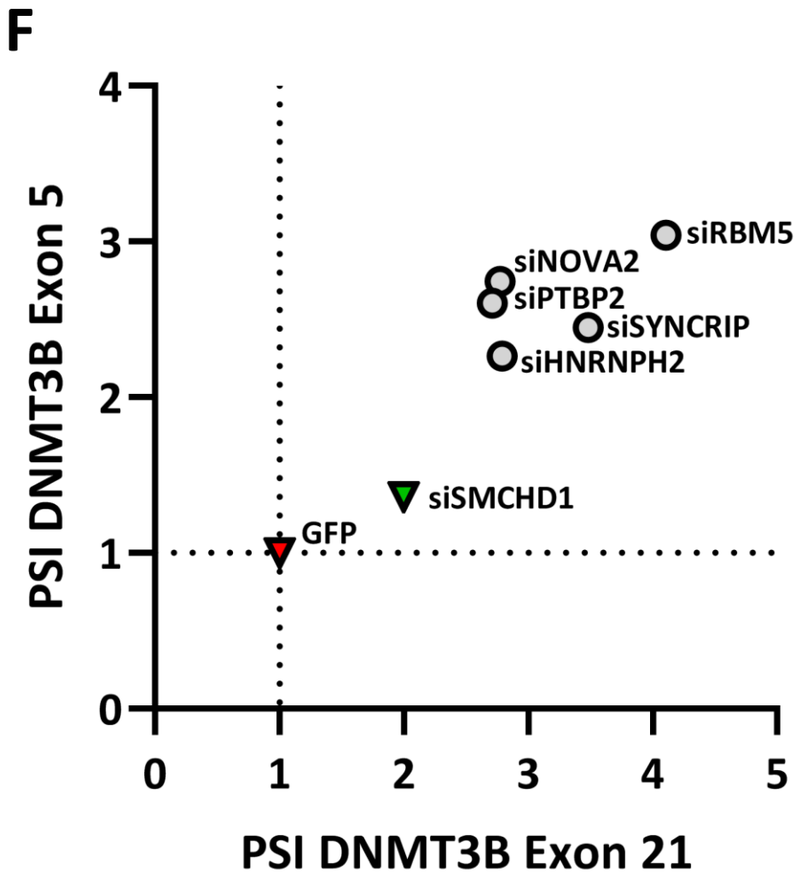

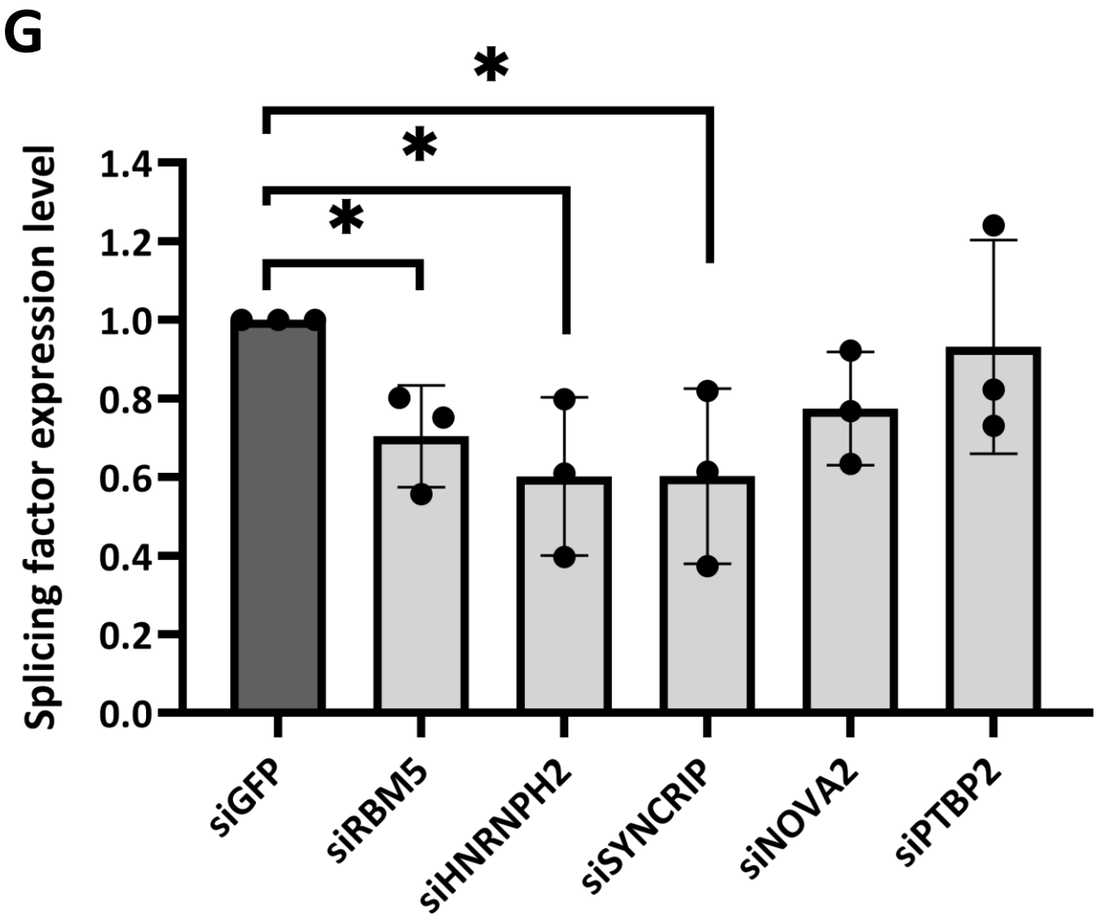

Figure S5

(A) RNA was extracted from three Smchd1^{MommeD1} mice NSC samples and two WT mice NSC samples. RNA-seq was conducted and analyzed using rMATS (FDR<0.05). Genome browser view of the Dnmt3b alternatively spliced junctions presented by sashimi plots, arcs denote splice junctions quantified in spanning reads. ***(B-D)*** HCT116 cells were transfected with siRNA targeting SMCHD1 or GFP as negative control. Total RNA was extracted and analyzed by real-time PCR for SMCHD1 total mRNA amount relative to *CycloA* reference gene. Values represent averages of three experiments done in triplicates ±SD normalized to negative control (siGFP) [****p<0.0001] (paired Student's t-test) **(B)**. Semi quantitative PCR was conducted for exons 4-5 **(C)** and exons 20-21 **(D)** using custom primers as described. PSI is calculated as the included product amount relative to the excluded product, and normalized to siGFP as a negative control. ***(E)*** HCT116 cells were treated with 6uM of CPT or DMSO as negative control for 6 hr. Total RNA was extracted and analyzed by real-time PCR for total DNMT3B mRNA amount relative to *CycloA* reference gene. Values represent averages of three experiments done in triplicates ±SD normalized to negative control (DMSO) [**p<0.01] (paired Student's t-test). ***(F)*** HCT116 cells were transfected with siRNA targeting 71 human splicing factor, SMCHD1 as a positive control and GFP as negative control. Total RNA was extracted and analyzed by real-time PCR for DNMT3B exon 5 and exon 21 relative to DNMT3B total mRNA amount. PSI was calculated as DNMT3B exon inclusion/DNMT3B total mRNA and normalized to negative control (siGFP). Values represent averages of two experiments ±SD. Negative control (siGFP) PSI is represented by the dotted line at 1. ***(G)*** HCT116 cells were transfected with siRNA targeting each splicing factor hit indicated or GFP as a negative control. Total RNA was extracted and analyzed by real-time PCR for splicing factor total mRNA amount relative to *CycloA* reference gene. Values represent averages of three experiments done in triplicates ±SD normalized to negative control (siGFP) [*p<0.05] (paired Student's t-test).

Figure S6

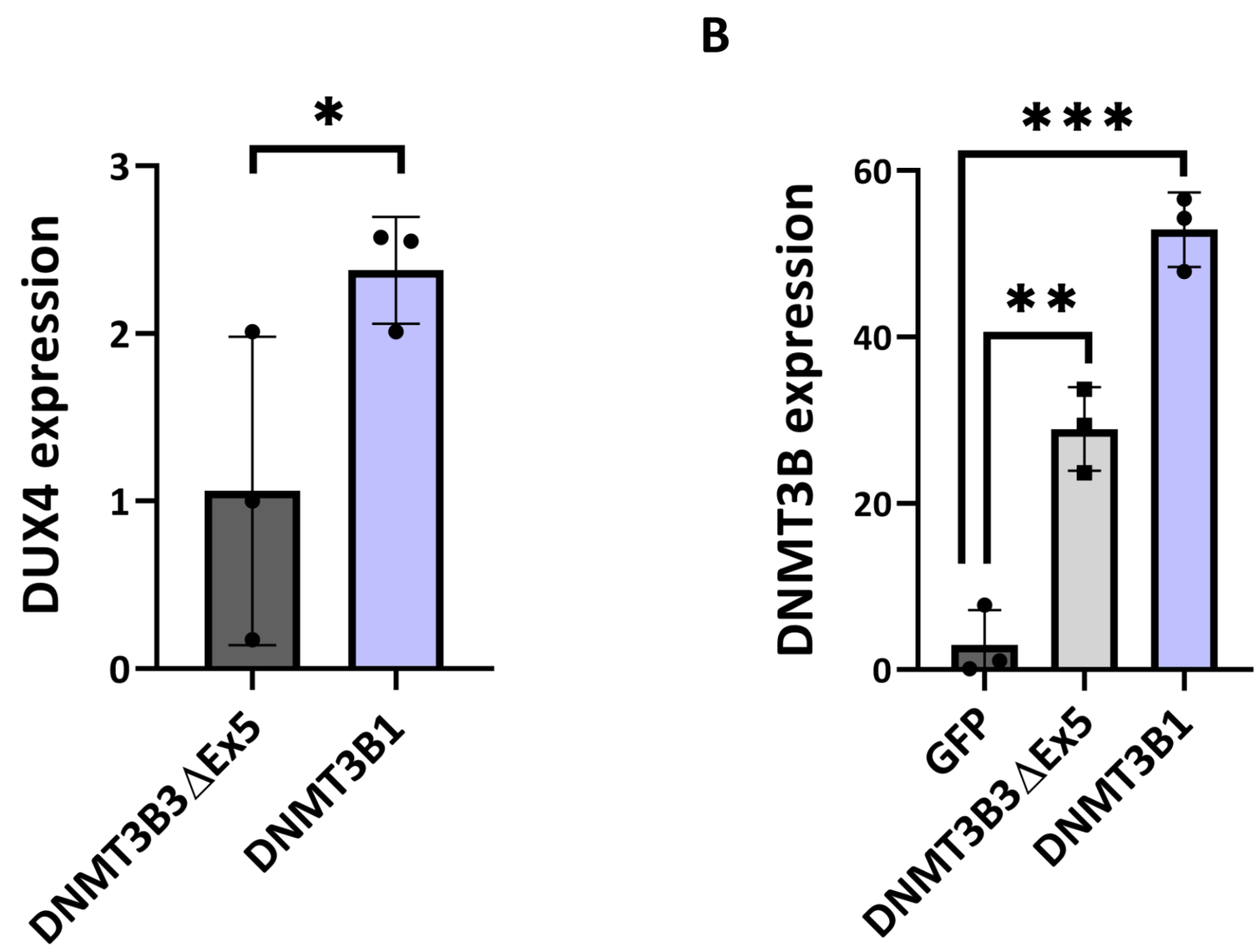

Figure S6

(A) RNA was extracted from HCT-116 cells with the DNMT3B3ΔEx5 and DNMT3B1 isoforms and real-time PCR was conducted. DUX4 mRNA level was quantified relative to *CycloA* reference gene. Values represent averages of three technical replicates ±SD; [* $p<0.05$] (Student's t-test). ***(B)*** Human skeletal myoblast cells were infected with lentiviruses containing empty-GFP, GFP-DNMT3B3ΔEx5 or GFP-DNMT3B1. To asses successful infection, Real-time PCR was conducted and DNMT3B mRNA level was quantified relative to *CycloA* reference gene. Values represent averages of three technical replicates ±SD; [** $p<0.01$; *** $p<0.001$] (Student's t-test).